

Neutralino Annihilations and the Gas Temperature in the Dark Ages

Zacharia Myers and Adi Nusser

Physics Department, Technion, Haifa 32000, Israel and the Asher Space Research Institute

2 February 2008

ABSTRACT

Assuming the dark matter is made entirely from neutralinos, we re-visit the role of their annihilation on the temperature of diffuse gas in the high redshift universe. We consider neutralinos of particle mass 36 GeV and 100 GeV, respectively. The former is able to produce $\sim 7 e^-e^+$ particles per annihilation through the fermionic channel, and the latter ~ 53 particles assuming a purely bosonic channel. High energy e^-e^+ particles up-scatter the Cosmic Microwave Background (CMB) photons into higher energies via the inverse-Compton scattering. The process produces a power-law e^-e^+ energy spectrum of index -1 in the energy range of interest, independent of the initial energy distribution. The corresponding energy spectrum of the up-scattered photons is a power-law of index $-1/2$, if absorption by the gas is not included. The scattered photons photo-heat the gas by releasing electrons which deposit a fraction (14%) of their energy as heat into the ambient medium. For uniformly distributed neutralinos the heating is insignificant. The effect is greatly enhanced by the clumping of neutralinos into dense haloes. We use a time-dependent clumping model which takes into account the damping of density fluctuations on mass scales smaller than $\sim 10^{-6} M_\odot$. With this clumping model, the heating mechanism boosts the gas temperature above that of the CMB after a redshift of $z \sim 30$. By $z \approx 10$ the gas temperature is nearly 100 times its temperature when no heating is invoked. Similar increase is obtained for the two neutralino masses considered.

Key words: cosmology: theory, observation, dark matter, large-scale structure of the Universe — intergalactic medium

1 INTRODUCTION

Early formation of luminous objects (stars, galaxies, mini-quasars) in the universe is governed by an intricate interplay between energetic (mechanical and radiative) feedback from these objects and the physical properties of the surrounding diffuse gas (e.g. Benson et al. 2006). Gas accretion onto dark matter (DM) haloes, and its cooling inside them, depend on its density and temperature which are greatly affected by feedback from the forming luminous objects (e.g. Benson et al. 2006, Thomas & Zaroubi 2007). However, before the onset of the first generation of luminous objects (e.g. Abel, Bryan, & Norman 2002; Bromm, Coppi, & Larson 2002) and with the exception of coupling to the CMB, energetic sources affecting the state of the diffuse gas^{*} could only be

associated with the dark matter through its decay, annihilation and direct collisions with ordinary matter. Direct collisions are relevant for super-heavy dark matter (particle mass $\sim 10^5 - 10^{15}$ GeV which does not violate bounds by ground experiments on the interaction cross section with baryons (Albuquerque & Baudis 2003). However, the cross section needed to heat the high redshift diffuse gas is about 10 orders of magnitude larger than the upper bound derived from clusters of galaxies (Chuzhoy & Nusser 2006). Various effects of dark matter decay and annihilation on the gas at high redshift and background radiations have been studied (Sciama 1982; Chen & Kamionkowski 2004; Hansen & Haiman 2004; Kasuya, Kawasaki, & Sugiyama 2004; Pieri & Branchini 2004; Pierpaoli 2004; Padmanabhan & Finkbeiner 2005; Kasuya & Kawasaki 2006; Mapelli et al. 2006; Furlanetto et al. 2006; Ullio et al. 2006; Zhang et al. 2006; Freese, Gondolo & Spolyar 2007; Ripamonti et al. 2007). Here we focus on heating the diffuse gas as a result of neutralino annihilations, taking into account their clumping into small

^{*} We avoid the term “intergalactic medium (IGM)” to refer to the gas at such high redshifts as it is unlikely that galaxies existed at those early times.

dense haloes (e.g. Green, Hofmann, & Schwarz 2005) and a detailed analysis of energy deposition into the gas. The main heating process is through inverse-Compton scattering (ICS) of CMB photons by e^-e^+ particles produced in the annihilations. The ICS process, involves the collision of a high-energy electron/positron and a low-energy photon, with consequent production of a high-energy recoil photon and a corresponding decrease in electron energy, (Felten and Morrison, 1966). Once in contact with the CMB, these DM e^-e^+ up-scatter the photons, shifting their energies to hard UV, X-ray and γ -ray levels. The heating effect from these up-scattered photons is only significant after DM clumping into (micro-) haloes of mass $\sim 10^{-6}M_\odot$ has begun. The annihilation rate, which is proportional to the DM density squared increases by orders of magnitude inside these dense haloes.

The neutralino, χ , is the lightest stable supersymmetric particle (See Jungman, Kamionkowski, and Griest 1996 for a review). While much is still unknown about neutralinos because it is difficult to detect them directly, they are considered to be Majorana fermions (and therefore are their own anti-particles, $\chi = \bar{\chi}$); thus, they self-annihilate and produce some combination of bosons, mesons, e^-e^+ pairs, and γ -rays (see Gunn et al. 1978 for the basic scenario). Baltz and Wai (2004) point out that a significant fraction of the power liberated in self-annihilation may go into high-energy e^+e^- pairs. Monochromatic electrons (with energy $\approx M_\chi$), coming from the direct channel $\chi\chi \rightarrow e^+e^-$, are generally suppressed (Turner and Wilczek 1990); electrons are then produced from the decay of the final heavy fermions and bosons. Low mass estimates for the neutralino such as 80 GeV or lower will not produce any bosons because they are too light. For estimates of $M_\chi = 100$ GeV or higher, DM annihilations produce bosons followed by a decay chain of subsequent particles including electrons.

The different composition of the $\chi\bar{\chi}$ annihilation final states will in general affect the form of the final e^-e^+ spectrum. Similar to Colafrancesco and Mele (2000), we consider two different cases: 1) a light mass neutralino, $M_\chi=36$ GeV, which yields mainly fermion pair production $\chi\bar{\chi} \rightarrow ff$, (Turner and Wilczek 1990); 2) a heavier neutralino, $M_\chi=100$ GeV annihilating into predominantly W (and Z) vector bosons, $\chi\bar{\chi} \rightarrow WW(ZZ)$. A real situation will be mostly reproduced by either of the above two cases, or by a linear combination of the two (Colafrancesco & Mele 2000). The e^-e^+ energy spectrum arising from the $\chi\bar{\chi}$ annihilation has been derived by various authors (Silk and Srednicki 1984, Rudaz and Stecker 1988, Ellis et al. 1989, Stecker and Tylka 1989, Turner and Wilczek 1990, Kamionkowski and Turner 1991, Baltz and Edsjo, 1998). Here, we adopt an approach similar to Rudaz and Stecker (1988) and Kamionkowski and Turner (1991), that gave the analytical approximations of the electron source functions for models in which neutralinos annihilate mainly into fermions and vector bosons, respectively. Given the source spectrum we can estimate the 'enhancement factor' N_{enh} defined as the number of e^-e^+ particles that are produced in a single neutralino annihilation.

Our notation is as follows. The scale factor of the universe is $a(t)$, the Hubble function is $H(z) = \dot{a}/a$, the critical

density is $\rho_{\text{crit}} = 3H^2/(8\pi G)$. The mass densities (in units of ρ_{crit}) corresponding to dark matter (i.e. neutralino), baryonic matter, dark energy (cosmological constant), and curvature are, respectively, Ω_M , Ω_B , are Ω_Λ and Ω_K . For the ratio, $h(z) = H(z)/H_0$, where $H_0 = H(z=0)$, we use

$$h(z) = \sqrt{\Omega_M(1+z)^3 + \Omega_K(1+z)^2 + \Omega_\Lambda}. \quad (1)$$

We consider a flat universe, $\Omega_K = 0$, with $\Omega_M = 0.24$, $\Omega_B = 0.04$, $\Omega_\Lambda = 0.72$ and $H_0 = 73 \text{ km s}^{-1} \text{ Mpc}^{-1}$ in accordance with Spergel et al. (2007).

The outline of the paper is as follows. In §2 we summarize the relevant equations used to obtain the enhanced temperature of the diffuse gas at high redshifts. In §3 we present the results of the calculations. We conclude in §4.

2 THE EQUATIONS

The annihilation by-product particles, e^-e^+ , inverse-Compton scatter CMB photons to high energies. The up-scattered photons (hereafter ICS photons) deposit part of their energy into the diffuse gas through the process of photo-ionization. Our goal is to compute the heating rate and the temperature of the gas as a function of time. The heating rate per baryon is given by

$$\mathcal{H}(z) = 4\pi f_{\text{heat}} \int_{E_{\text{ion}}} \frac{J(E_{\text{ph}}, z)}{E_{\text{ph}}} (E_{\text{ph}} - E_{\text{ion}}) \sigma_{\text{ion}}(E_{\text{ph}}) dE_{\text{ph}}, \quad (2)$$

where $J(E_{\text{ph}})$ is the energy flux of the ICS photons in units of $\text{MeV cm}^{-2} \text{ sr}^{-1} \text{ s}^{-1} \text{ MeV}^{-1}$, $E_{\text{ion}} = 13.6 \text{ eV}$ is the H I ionization energy, and $\sigma_{\text{ion}} = 6 \times 10^{-18} (E_{\text{ph}}/E_{\text{ion}})^3 \text{ cm}^2$ for $E_{\text{ph}} > E_{\text{ion}}$ and zero otherwise. The factor f_{heat} is the fraction of energy of released electrons which is deposited as heat by collisions with the gas particles (atoms and free thermal electrons). This factor depends strongly on the ionization fraction of the gas, ranging from almost unity for nearly fully ionized gases to $f_{\text{heat}} \approx 0.135$ for an ionization fraction of 10^{-4} (Shull & Van Steenberg 1985). We ignore the mild dependence of f_{heat} on the electron energy and consider its lower limit values which are obtained for very high electron energies. The residual ionized fraction from the epoch of recombination is $\approx 2 \times 10^{-4}$ (e.g. Peebles 1993), which gives the value $f_{\text{heat}} = 0.144$ (Shull & Van Steenberg 1985) adopted in this work. The ICS energy flux, $J(E_{\text{ph}})$, is given by (e.g. Haardt & Madau, 1996),

$$J(E_{\text{ph}}, z) = \frac{1}{4\pi} \frac{c}{H_0} \int_z^{z_{\text{rec}}} \frac{d\tilde{z}}{(1+\tilde{z})h(\tilde{z})} \epsilon(\tilde{E}_{\text{ph}}, \tilde{z}) e^{-\tau(E_{\text{ph}}, z, \tilde{z})} \quad (3)$$

where c is the speed of light, $\tilde{E}_{\text{ph}} = E_{\text{ph}}(1+\tilde{z})/(1+z)$, and ϵ is the emissivity (in units of $\text{MeV per s MeV cm}^3$) of ICS radiation per unit volume comoving with respect to an observer at redshift z , i.e., the emissivity per unit proper volume is $(1+z)^3/(1+\tilde{z})^3 \epsilon$. In the above expression, no contribution from e^-e^+ generated from annihilations before the epoch of recombination at $z_{\text{rec}} \approx 1000$ is taken into account. The reason is that the mean free path of such e^-e^+ particles is so small that they are thermalised with the cosmic plasma before they escape to lower redshifts. The optical depth for

absorption is

$$\tau(E_{\text{ph}}, z, \tilde{z}) = \frac{c}{H_0} \int_z^{\tilde{z}} \frac{dz'}{(1+z')h(z')} \sigma_{\text{ion}}(E'_{\text{ph}}) n_{\text{H}}(z') \quad (4)$$

where $n_{\text{H}}(z') \approx 1.8 \times 10^{-7} \text{cm}^{-3} (1+z')^3$ is the proper H I density at redshift z' and $E'_{\text{ph}} = E_{\text{ph}}(1+z')/(1+z)$. Here we consider absorption only by H I.

The ICS emissivity depends on the CMB temperature $T_{\text{CMB}}(z) \approx 2.73(1+z)\text{K} = 2.3 \times 10^{-10}(1+z) \text{MeV}/k_{\text{B}}$ (where k_{B} is Boltzmann constant), its energy density $U = 2.6 \times 10^{-7}(1+z)^4 \text{MeV cm}^{-3}$, and the number density of e^-e^+ as a function of energy. The expression for $\epsilon(E_{\text{ph}}, z)$ as a function of the photon energy is (Felten & Morrison 1966),

$$\epsilon(E_{\text{ph}}, z) = \frac{P(\gamma_{E_{\text{ph}}}, U) N(\gamma_{E_{\text{ph}}})}{7.2(k_{\text{B}} T_{\text{CMB}}) \gamma_{E_{\text{ph}}}}. \quad (5)$$

In this expression, it is assumed that only electrons/positrons with a Lorentz factor of

$$\gamma_{E_{\text{ph}}} = \left(\frac{E_{\text{ph}}}{3.6kT_{\text{CMB}}} \right)^{1/2} \quad (6)$$

contribute to the ICS flux of photons at energy E_{ph} . Further, $P(\gamma, U)$ is the inverse-Compton power scattered by one electron and is given by (Felten & Morrison 1966)

$$P(\gamma, U) = \frac{4}{3} \sigma_{\text{T}} c \gamma^2 U, \quad (7)$$

where $\sigma_{\text{T}} = 6.65 \times 10^{-25} \text{cm}^2$ is the Thomson cross-section, and $N(\gamma)d\gamma$ gives the comoving (with respect to an observer at redshift z) number density of e^-e^+ particles with Lorentz factors in the range $\gamma \rightarrow \gamma + d\gamma$.

2.1 The electron energy distribution

The energy distribution function $N(\gamma, z)$ of e^-e^+ particles is determined by the energy losses they incur through ICS with the CMB. For simplicity, we assume here that all electrons are produced with the same energy E_0 , corresponding to a Lorentz factor of $\gamma_0 = E_0/m_e c^2$ ($m_e c^2$ is the electron mass). Although the generalization to a general initial source spectrum is straightforward, we will see that the evolved spectrum is insensitive to the details of the initial spectrum.

The production rate of electrons per unit volume (which is comoving with an observer at redshift zero[†]) is

$$\frac{dN_{e^-e^+}}{dt} = N_{\text{enh}} (n_{\chi}(z))^2 \langle \sigma v \rangle (1+z)^{-3}, \quad (8)$$

where $n_{\chi}(z) = \Omega_{\text{M}} \rho_{\text{crit}}/M_{\chi} \propto (1+z)^3$ is the proper neutralino number density at redshift z and N_{enh} is 7.6 and 53.2 for electrons produced from fermionic and bosonic decay chains, respectively. The annihilation cross section is $\langle \sigma v \rangle = 2 \times 10^{-26} \text{cm}^3 \text{s}^{-1}$ (e.g. Finkbeiner 2005).

[†] This rate can be transformed to a unit volume which is comoving with observers at redshift z_1 by a multiplication with $(1+z_1)^3$.

The energy loss rate of an electron as a result of scattering with the CMB is given by

$$\frac{d\gamma}{dt} = -\frac{P(\gamma)}{m_e c^2}. \quad (9)$$

Taking P from equation (7) yields,

$$\frac{d\gamma}{dt} = -A\gamma^2(1+z)^4, \quad (10)$$

where $A = 2.7 \times 10^{-20} \text{s}^{-1}$. The e^-e^+ particles can also lose energy by direct collisions with the gas. The corresponding energy loss rate is $d\gamma/dt|_{\text{coll}} = \gamma c n_{\text{H}} \sigma_{\text{eH}} = 3 \times \ln(\gamma) 10^{-15} [(1+z)/10]^3 \text{s}^{-1}$ where σ_{eH} is the cross section for direct collisions (Shull & Van Steenger 1985). By comparing with (10) we see that direct collisions are more important than ICS losses for Lorentz factors $\gamma < \gamma_{\text{coll}} \approx 4(\ln \gamma)^{1/2} [(1+z)/10]^{-1/2}$. The fraction of energy in e^-e^+ particles with $\gamma < \gamma_{\text{coll}}$ relative to the total energy produced by annihilations is $\sim \gamma m_e c^2 / M_{\chi} < 10^{-4}$. This is to be compared with the fraction of energy in electrons released by ICS photons. This fraction is $\sim 5\%$ as we shall see below. Thus heating through direct collisions of e^-e^+ particles with the gas is negligible.

The comoving number density (with respect to an observer at redshift zero) $N(\gamma, z)$ is related to the production rate in equation (8) by

$$N(\gamma, z) d\gamma = \frac{dN_{e^-e^+}(z_p)}{dt} dt_p, \quad (11)$$

where $z_p(\gamma)$ is the redshift at which an e^-e^+ particle with Lorentz factor γ (currently present at z) is produced and dt_p is the difference in the production times of electrons with γ and $\gamma + d\gamma$. The redshift z_p is determined by equation (10) with the initial condition that the electron is produced with γ_0 . Together with the equations (8), (10), the relation (11) yields,

$$N(\gamma, z) = \frac{N_0}{(1+z_p)\gamma^2} \quad (12)$$

where

$$N_0 = \frac{N_{\text{enh}}}{A} n_{\chi}^2 \langle \sigma v \rangle. \quad (13)$$

At high redshifts, $(1+z) \propto t^{-2/3}$ and the energy loss equation (10) gives $z_p(\gamma)$ in terms of

$$(1+z_p)^{5/2} = \frac{5}{2} \Omega_{\text{m}} H_0 \left(\frac{1}{A\gamma} - \frac{1}{A\gamma_0} \right) + (1+z)^{5/2}. \quad (14)$$

For the relevant γ values, this relation gives z_p . For an electron production energy of about $E_0 \lesssim 1 \text{GeV}$ we have $H_0/(A\gamma_0) \sim 0.04$ which is much smaller than $(1+z)^{5/2}$ at high z . Therefore, as long as γ is such that $H_0/(A\gamma) \ll (1+z)^{5/2}$ is satisfied we get z_p very close to z and $N(\gamma) \sim \gamma^{-2}$. Note that apart from setting an upper limit on the γ , the value of γ_0 affects neither the shape nor the amplitude of $N(\gamma)$ below that limit. For $H_0/(A\gamma) \gg (1+z)^{5/2}$ we have $z_p \propto \gamma^{-2/5}$ which gives $N(\gamma) \propto \gamma^{-8/5}$, instead of γ^{-2} . However, at $z \gtrsim 10$, for e^-e^+ energies spanning the range $1 - 10^3 \text{MeV}$, we find that $z_p = z$ to within a few percent.

So far, we have assumed that neutralinos are distributed uniformly with a number density of $n_{\chi} = \bar{\rho}/M_{\chi}$, where $\bar{\rho} = \Omega_{\text{M}} \rho_{\text{crit}}$ is the mean background density. The annihilation rate at a point \mathbf{x} in space is proportional to the square of

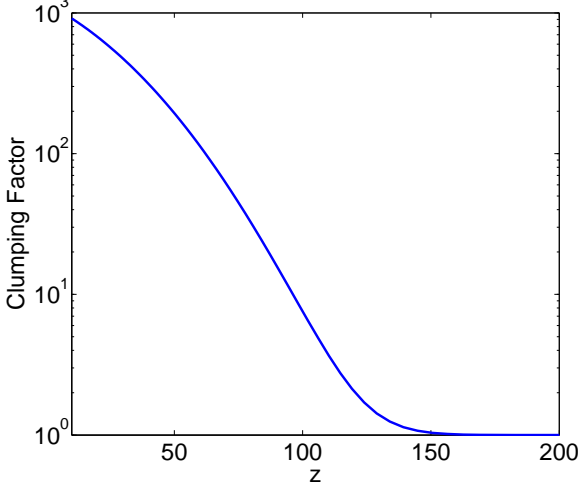


Figure 1. The neutralino clumping factor, f_{cl} , as a function of redshift.

the density, $\rho(\mathbf{x})$. Hence, clumping of neutralinos increases the mean annihilation rate by the factor $f_{\text{cl}} = \langle \rho(\mathbf{x}) / \bar{\rho} \rangle^2$ which is the variance of mass density fluctuations. Fluctuations in the neutralino distribution are damped below a mass scale of $M_d \sim 10^{-6} M_\odot$ because of neutralino collisions and free streaming (Green, Hofmann, & Schwarz 2005). We define a nonlinear clustering scale, M_{nl} by $\sigma_\delta(M_{\text{nl}}, z) = 1$, where $\sigma_\delta(M, z)$ is the rms value of density fluctuations smoothed with a top-hat window on the mass scale M . For sufficiently high redshifts we have $\sigma_\delta(M_{\text{nl}}, z) \ll M_d$ and no significant clumping is obtained. The mass fluctuations over a given mass scale grow with time and hence, M_{nl} will exceed M_d at some redshift. When this occurs, neutralinos begin to cluster into the first generation of haloes (of mass $> M_d$) and the clumping factor, f_{cl} , becomes significant. To compute f_{cl} at any redshift, we proceed as follows. If the fraction of mass in haloes is $F_h(z)$ then $f_{\text{cl}} = (1 - F_h) + F_h S$ where S depends on the density profile of the halo. Using the parametric form which matches the density profiles in simulations of first generation haloes (Diemand, Moore & Stadel 2005) gives $S = 1200$. Further, we estimate $F_h(z)$ according to the Press-Schechter (Press & Schechter 1974) cumulative mass function for the fraction of mass in haloes with mass larger than M_d where we assume that $M_d = M_{\text{nl}}$ at $z = 60$ (e.g. Pieri et al. 2007; Green, Hofmann & Schwarz 2005). The clumping factor is plotted in figure (1).

3 RESULTS

3.1 The electron spectrum

In figure (2) we plot, $N/m_e c^2$, i.e. the number density of $e^- e^+$ particles per unit energy as a function of the particle energy. The upper and lower panels correspond to neutralino masses of 36 GeV and 100 GeV, respectively. In each panel the spectra at redshifts, $z = 50, 30, 20$ and 10 are shown. Only annihilations at redshifts $z < 1000$ are considered. A

slope of -2 describes all curves extremely well. The transition to $-8/5$ is almost undetectable down to energies close to the rest mass of the electron. For $M_\chi = 36$ GeV the fermionic channel is applicable and for $M_\chi = 100$ GeV we assume a purely bosonic channel. While electron number density scales as $1/M_\chi^2$ (see eq. 13), the light ($M_\chi = 36$ GeV) and heavy ($M_\chi = 100$ GeV) neutralinos produce similar heating rates. This is because the heavy neutralino is assumed to produce $e^- e^+$ through the bosonic decay chains which yield a larger enhancement factor ($N_{\text{enh}} \sim 53$) than the fermionic channel ($N_{\text{enh}} \sim 7$) responsible for $e^- e^+$ production through annihilations of the lighter particle.

3.2 The spectrum of ICS photons

Given the energy distribution $N(\gamma)$, the spectrum of the ICS photons can readily be computed at any redshift using the expression (3). In figure (3) we show, $J(E_{\text{ph}})/E_{\text{ph}}$, i.e. number flux of ICS photons. The energy range extends to much higher energies, but we plot the flux only for the range which is relevant for heating the gas. Substituting the relations (12) and (5) in (3) we obtain $J/E_{\text{ph}} \propto E_{\text{ph}}^{-1.5}$ for $\tau = 0$. This behaviour is clearly seen in the curves corresponding to $\tau = 0$. When photo-ionization losses are included, a deep dip occurs at 1.36×10^{-5} MeV - the ionization energy threshold for hydrogen. The dip does not get down to zero due to ICS photons up-scattered during a time period of $\delta t_{\text{ion}} = 1/(c n_H \sigma_0) \sim (1+z)^{-3.5}$ Myr preceding z , the redshift at which J is given. Photo-ionization losses disappear at sufficiently high photon energies because of the decrease of the ionization cross-section with increasing energy ($\sigma_{\text{ion}} \propto E_{\text{ph}}^{-3}$). The amplitude of the spectrum is larger at higher redshifts. This is to be expected given the hotter, denser, CMB at higher redshifts. The dip extends from E_{ion} up to 1 keV. This is also the range of the kinetic energies of the released primary electrons. A detailed calculation gives a primary electron mean energy of ~ 50 eV.

3.3 The heating rates and the gas temperature

The gas temperature is governed by the energy equation,

$$\frac{dT}{dt} = \mathcal{H} - 2 \frac{\dot{a}}{a} T + \frac{T}{t_{\text{Compt}}}, \quad (15)$$

where \mathcal{H} is the heating rate by ICS photons, as given in (2), the second term on the right is adiabatic cooling of perfect gas at mean cosmic density, and the last term describes energy transfer between the CMB and the gas via Compton scattering of CMB photons with thermal free electrons. The time-scale, t_{Compt} (Peebles 1968) is,

$$t_{\text{Compt}} = \frac{1161.3(1+y^{-1})}{(1+z)^4[1 - T_{\text{CMB}}(z)/T]} \text{Gyr}. \quad (16)$$

In this expression, the ionization fraction, y , obeys the equation

$$\frac{dy}{dt} = \mathcal{I} - \alpha(T) y^2 n_H(z), \quad (17)$$

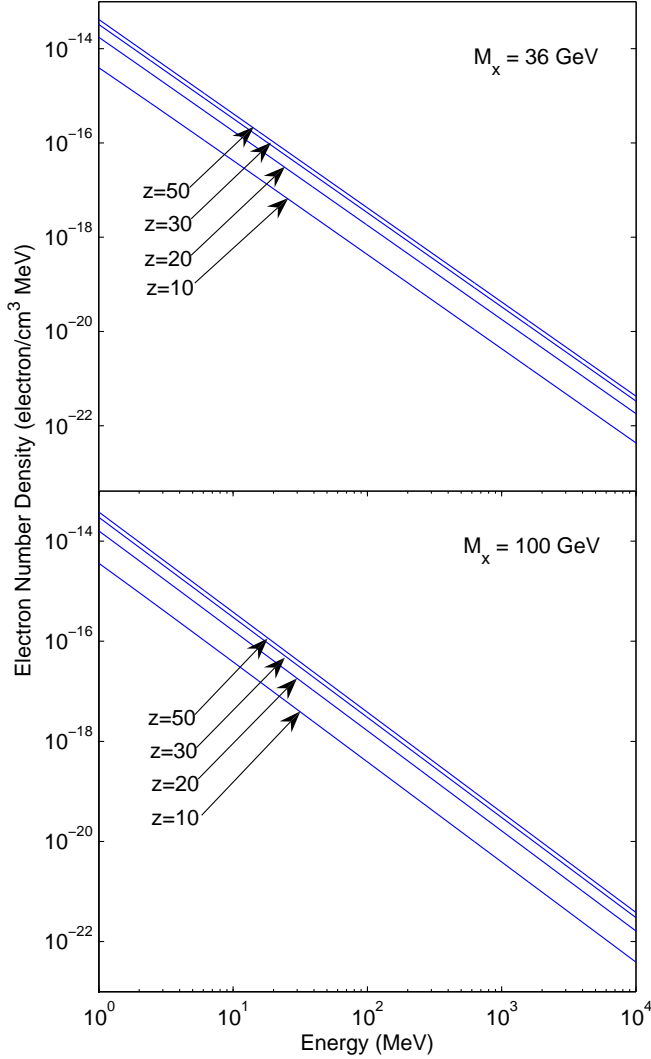


Figure 2. Spectra of e^-e^+ particles, resulting from IC losses to CMB photons, for neutralino masses of $M_\chi = 36$ GeV (top) and 100 GeV (bottom). Each panel shows spectra computed for 4 redshifts as indicated. Only annihilations below redshift 1000 are considered.

where $\alpha = 6.3 \times 10^{-11} T^{-1/2} (T/10^3)^{-0.2} / (1 + (T/10^6)^{0.7}) \text{ s}^{-1}$ (T in K) is the recombination rate and

$$\mathcal{I} = 4\pi \int_{E_{\text{ion}}} \frac{J}{E} \left[1 + f_{\text{ion}} \left(\frac{E}{E_{\text{ion}}} - 1 \right) \right] \sigma_{\text{ion}}(E) dE, \quad (18)$$

which includes contributions from two processes: direct ionization by ICS photons and from secondary electrons created by the primary energetic electron released by the first process. Ionizations by secondary electrons consume a fraction f_{ion} of the energy of primary electrons. There is a dependence on f_{ion} on y , but is rather weak at the relevant y values we get here. We simply take $f_{\text{ion}} = 0.36$ corresponding to an ionization fraction of 2×10^{-4} (Shull & Van Steenberg 1985).

The top panel of figure (4) shows the heating rate of the gas as a function of redshift. The rates include clumping according to the scheme described at the end

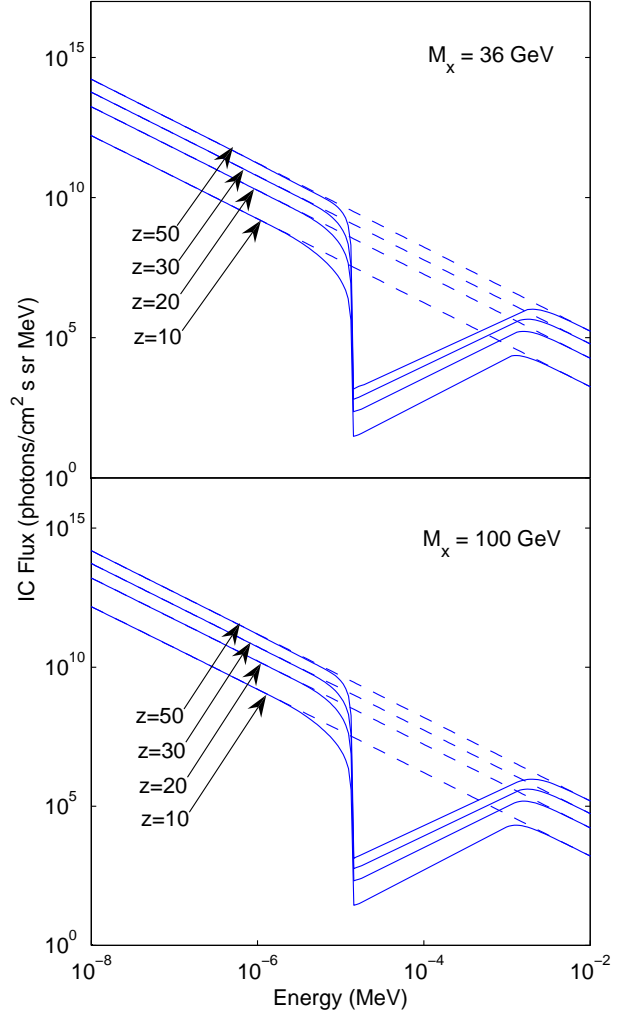


Figure 3. Spectra of ICS photons at difference redshifts, for $M_\chi = 36$ GeV (top) and $M_\chi = 100$ GeV (bottom). The solid line represents the ICS spectrum accounting for photon loss to H I ionizations; hence the noticeable dip. The dashed line is the spectrum without accounting for the loss to ionization.

of §2.1. It is interesting to compare this rate to the total energy rate produced by dark matter annihilations, i.e. $\langle \sigma v \rangle [n_\chi(z)]^2 M_\chi f_{\text{cl}}(z) / n_{\text{H}}(z)$. This ratio gives the heating efficiency of the ICS photons. The ratio, plotted in figure (5), is fairly constant for $z > 30$ at the level of 4%, but increases up-to 7% towards $z = 10$. The ionization rates, seen in the bottom panel, are too small to significantly increase the ionization fraction above its residual value from the epoch of recombination. A numerical solution of the ionization equation (17) yields a maximum ionization fraction of $\sim 10^{-3}$ which is obtained at the lowest redshifts considered here, $z \sim 10$.

Given the heating and ionization rates, we numerically solve equations (15) and (17) to obtain the gas temperature as a function of redshift. Figure (6) shows numerical solutions with the initial condition $T = T_{\text{CMB}}$ at $z = 500$. The dash-dotted curve representing $T(z)$ with no heating is ob-

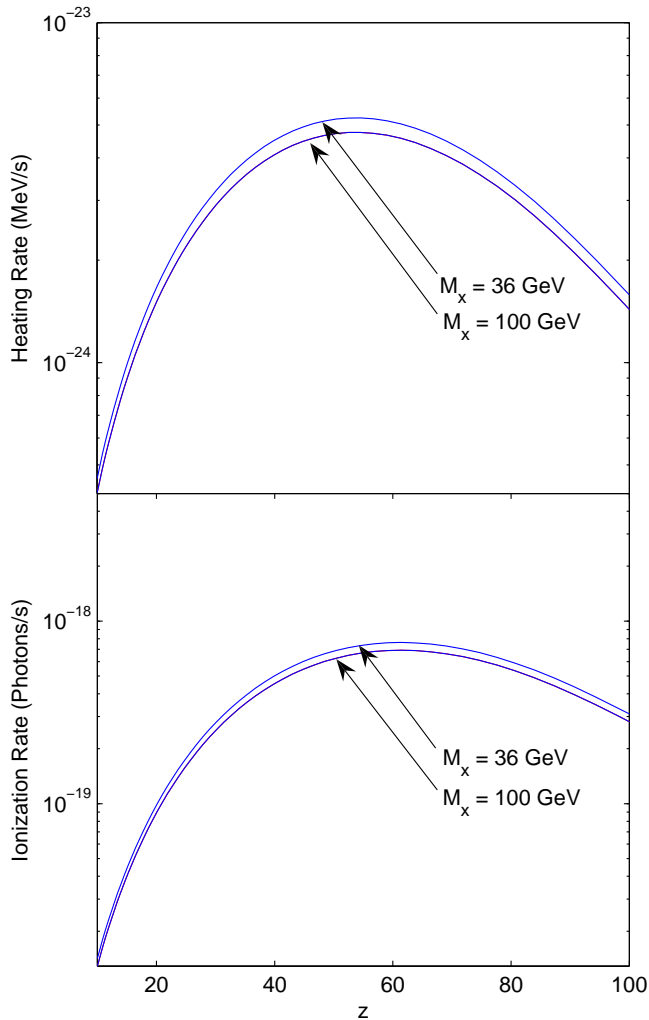


Figure 4. The heating (top panel) and ionization (bottom) rates as a function of redshift for $M_\chi = 36$ GeV and $M_\chi = 100$ GeV as indicated in the figure.

tained assuming $y = 2 \times 10^{-4}$ at all redshifts. Nonetheless, Compton coupling (heating in this case) plays no role at the plotted redshift range as the curve with no heating declines as $(1+z)^2$ as expected from adiabatic cooling alone. The CMB temperature (dashed curves) follows $(1+z)$ and it is above the gas temperature when heating is not invoked. The solid curves in the two top panels are the temperature when ICS heating is included. Both neutralino masses yield similar gas temperatures. The rise in the gas temperature at $z > 30$ is significant, but is not enough to bring the gas above T_{CMB} . At $z < 30$ the heated gas temperature exceeds the T_{CMB} .

4 CONCLUSIONS

The heating of the gas by neutralino annihilations is mediated by CMB photons up-scattered by collisions with energetic e^-e^+ particles generated as a by-product of the anni-

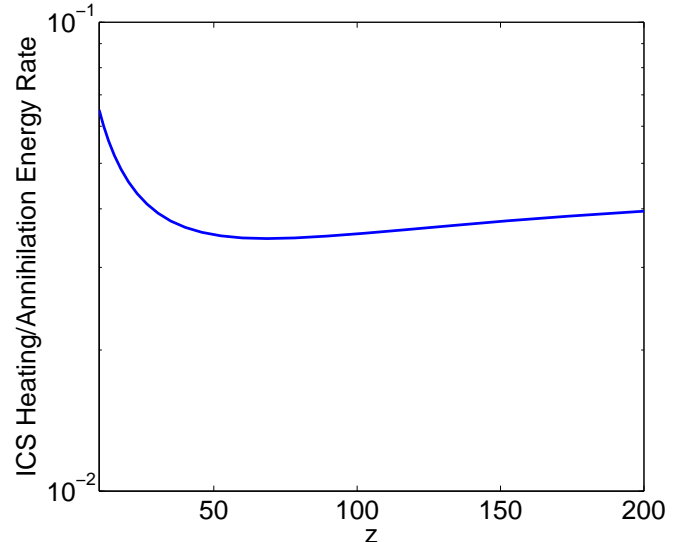


Figure 5. The ratio of the gas heating by ICS photons to the rate of total energy released in DM annihilations.

hilation. Significant heating is obtained due to the clumping neutralinos into haloes. Since the heating rate is directly proportional to the clumping factor, comparison between the figures (1), (4) and (6) reveals that only negligible heating could be achieved if clumping is not included. The simple clumping model we adopt here could be improved to account for the dependence of halo profile on redshift and mass. These effects may enhance the clumping factor, yielding a more significant heating rate. A more precise model of the clumping factor could be achieved by additional high resolution simulations of the early stages of neutralino clustering.

It is interesting to see how patchy the ICS heating is when the mass fraction in haloes is small. Electrons/positrons produced in a single halo, will travel some distance away from their origin before their energy becomes low enough so that the corresponding ICS photons are capable of ionizing H I. The degree of patchiness could be assessed by a comparison of this distance with the mean separation between haloes. According to (6), an electron (or positron) with Lorentz factor γ up-scatters a CMB photon to energy (in eV) $E_{\text{ph}} = 8.2 \times 10^{-4} \gamma^2 (1+z)$. Therefore, $\gamma \sim 40$ is needed to bring a $z = 10$ CMB photon at to $\sim E_{\text{ion}} = 13.6$ eV, the H I ionization threshold. The time it takes an electron to lose energy from its initial value $\gamma_0 \gg 40$ down to $\gamma \ll \gamma_0$ is $[\gamma A(1+z)^4]^{-1}$ which gives 2.3 Myr for our photon of $\gamma \sim 40$ at $z \sim 10$. The comoving distance travelled by the electron during this time is ~ 10 Mpc. This is huge compared to the mean separation, $3F_h^{-1/3}$ pc, between haloes of mass $\sim 10^{-6} M_\odot$, unless the mass fraction, F_h is extremely small. Therefore, the ICS photons form a uniform background.

The temperature increase could be significant for determining the onset of galaxy formation. A temperature T corresponds to a potential depth of a halo of mass,

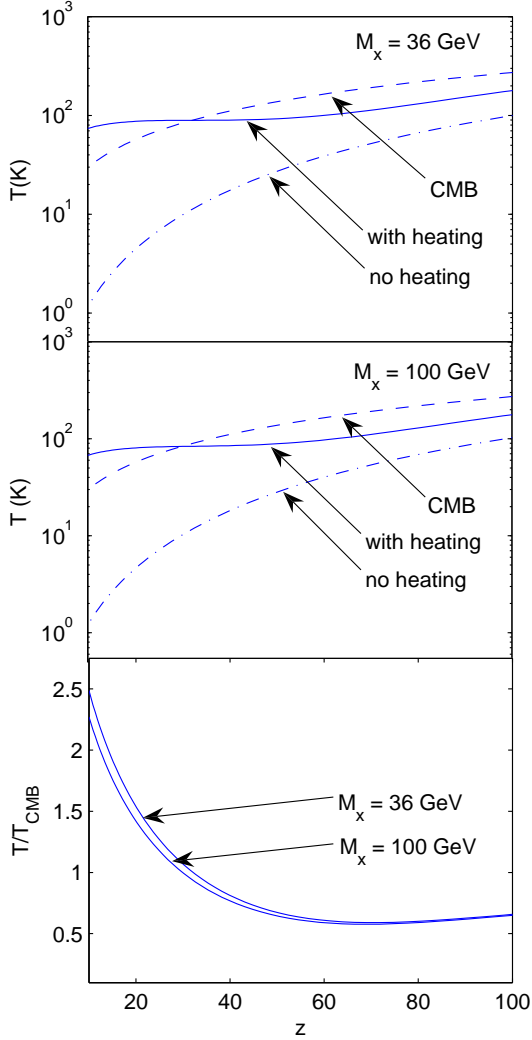


Figure 6. Top and middle panels show temperature of diffuse gas with and without heating, as a function of redshift. Plotted also is the temperature of the CMB. The bottom panel shows the ratio of the heated gas temperature relative to that of the CMB.

$M = \frac{20}{1+z} (\frac{T_v}{10^9})^{3/2} 10^9 M_\odot$ for $\Omega_M \approx 1$ as is the case at high redshifts. A gas at temperature T could only be gravitationally trapped by haloes with T_v greater than T . For a gas cooling adiabatically without any heating mechanism we get $T = 10\text{K}$ at $z \approx 20$. Therefore, gas can collapse onto haloes of mass $> 10^3 M_\odot$. At this redshift, the heating mechanism described here, boosts the temperature of the gas by a factor of 10 at $z \approx 20$ which raises its mass threshold for collapse to $3 \times 10^4 M_\odot$. This change in the mass threshold could result in a significant delay in the onset of star/galaxy formation.

The temperature increase could be relevant for observations of 21 cm radiation from H I at high redshifts. The 21 cm differential brightness temperature is $\delta T_b \approx 16\text{mK}(1+\delta)[(1+z)/10]^{1/2}(T_s - T_{\text{CMB}})/T_s$ where δ is the gas density contrast. Collisional coupling (e.g. Field 1959) of the kinetic and spin temperatures of the gas could boost the latter above T_{CMB} . An estimate of this coupling gives

$(T_s - T_{\text{CMB}})/T_s \approx 0.1$ at $z \approx 20$ for a density contrast of unity which gives $\delta T_b \approx 4\text{mK}$. This is not far from the sensitivity of planned 21 cm experiments.

ACKNOWLEDGEMENTS

This research is supported by the German-Israeli Science Foundation for Development and Research and by the Asher Space Research fund. ZM wishes to thank the Israeli Ministry of the Absorption of Science for providing the research funds necessary to support this work.

REFERENCES

- Abel T., Bryan G. L., Norman M. L., 2002, *Sci*, 295, 93
- Albuquerque I.F.M, Baudis L., 2003, *PhRvL*, 91, 9903
- Baltz, E.A. and Edsjo 1998, preprint astro-ph/9808243
- Baltz, E. A. and Wai, L. 2004, astro-ph/0403528
- Benson A. J., Sugiyama N., Nusser A., Lacey C. G., 2006, *MNRAS*, 369, 1055
- Bromm V., Coppi P. S., Larson R. B., 2002, *ApJ*, 564, 23
- Chen X., Kamionkowski M., 2004, *PhRvD*, 70, 043502
- Chuzhoy L., Nusser A., 2006, *ApJ*, 645, 950
- Colafrancesco, S., and Mele, B., 2001, *ApJ*, 562, 24-41
- Diemand J., Moore B., Stadel J., 2005, *Nature*, 433, 389
- Ellis, J. et al. 1989, *Phys. Lett. B*, 214, 403
- Felten J. E., Morrison P., 1966, *ApJ*, 146, 686
- Field G. B., 1959, *ApJ*, 129, 536
- Finkbeiner, D., 2005, arXiv:astro-ph/0409027
- Freese K., Gondolo P., Spolyar D., 2007, astro-ph/0709.2369
- Furlanetto S. R., Oh S. P., Pierpaoli E., 2006, *PhRvD*, 74, 103502
- Green A. M., Hofmann S., Schwarz D. J., 2005, *JCAP*, 8, 3
- Gunn, J. E., Lee, B. W., Lerche, I., Schramm, D. N., and Steigman, G. 1978, *ApJ*, 223, 1015
- Hansen S. H., Haiman Z., 2004, *ApJ*, 600, 26
- Haardt, F., and Madau, P., 1996, *ApJ*, 461, 20
- Jungman, G., Kamionkowski, M., and Griest, K., 1996, *Physics Reports*, 267, 195
- Kamionkowski, M. and Turner, M.S., 1991, *Phys. Rev. D*, 43, 1774
- Kasuya S., Kawasaki M., Sugiyama N., 2004, *PhRvD*, 69, 023512
- Kasuya S., Kawasaki M., 2006, *PhRvD*, 73, 063007
- Mapelli M., Ferrara A., Pierpaoli E., 2006, *MNRAS*, 369, 1719
- Padmanabhan N., Finkbeiner D. P., 2005, *PhRvD*, 72, 023508
- Peebles P. J. E., 1968, *ApJ*, 153, 1
- Peebles P. J. E., 1993, *Principles of Physical Cosmology*, Princeton Series in Physics, Princeton, NJ: Princeton University Press
- Pieri L., Bertone G., Branchini E., 2007, arXiv, 706, arXiv:0706.2101
- Pieri L., Branchini E., 2004, *PhRvD*, 69, 043512
- Pierpaoli E., 2004, *PhRvL*, 92, 031301
- Press W. H., Schechter P., 1974, *ApJ*, 187, 425
- Ripamonti E., Mapelli M., Ferrara A., 2007, *MNRAS*, 374, 1067
- Rudaz, S. and Stecker, F.W. 1988, *ApJ*, 325, 16
- Sciamia D. W., 1982, *MNRAS*, 198, 1P
- Shull J. M., van Steenberg M. E., 1985, *ApJ*, 298, 268
- Silk, J. and Srednicki, M., 1984, *Phys.Rev.Lett.*, 53, 624
- Spergel D. N., et al., 2007, *ApJS*, 170, 377
- Stecker, F. and Tylka, A., 1989, *ApJ*, 336, L51
- Thomas R. M., Zaroubi S., 2007, arXiv, 709, arXiv:0709.1657
- Turner, M. and Wilczek, F. 1990, *PhRvD*, 42, 1001

Ullio P., Bergström L., Edsjö J., Lacey C., 2002, PhRvD, 66,
123502
Zhang L., Chen X., Lei Y.-A., Si Z.-G., 2006, PhRvD, 74, 103519